



ELSEVIER

Available online at www.sciencedirect.com

ScienceDirect

Transportation Research Procedia 00 (2018) 000–000

Transportation
Research
Procedia
www.elsevier.com/locate/procedia

International Symposium of Transport Simulation (ISTS'18) and the International Workshop on Traffic Data Collection and its Standardization (IWTDCS'18)

A modified particle swarm optimization algorithm to distribute lane changes in a freeway weaving segment

David Sulejic^{a,*}, Nasser R Sabar^b, Edward Chung^c

^aQueensland University of Technology, Brisbane QLD 4000, Australia

^bLa Trobe University, Bundoora VIC 3086, Australia

^cHong Kong Polytechnic University, Hung Hom, Hong Kong

Abstract

This paper presents an algorithm, based on particle swarm optimisation, to optimise the lane-changing distributions at a freeway weaving segment using an individual driver advisory. The research applies a microscopic simulation in Aimsun to evaluate the optimised lane-changing distribution for a one-sided freeway weaving segment. The simulation results show that the proposed particle swarm optimisation algorithm can be used as a successful optimisation method for the lane-changing distributions. The individual driver advisory, using the optimised lane-changing distributions, effectively distributes lane changes along the freeway weaving segment to improve the performance. The evaluation revealed that the proposed strategy has the potential to reduce delay, to increase traffic speed and smooth traffic flow dynamics.

© 2018 The Authors. Published by Elsevier Ltd.

This is an open access article under the CC BY-NC-ND license (<https://creativecommons.org/licenses/by-nc-nd/4.0/>)

Peer-review under responsibility of the scientific committee of the International Symposium of Transport Simulation (ISTS'18) and the International Workshop on Traffic Data Collection and its Standardization (IWTDCS'18)".

Keywords: particle swarm optimisation; freeway weaving segment; individual driver advisory

1. Introduction

Empirical studies have shown that drivers tend to perform lane changes soon after they enter the weaving segment, especially under capacity conditions (Cassidy and May, 1991; Kwon *et al.*, 2000; Denny and Williams, 2005; Lee, 2008; Al-Jameel, 2013; He and Menendez, 2016). This behaviour, known as the lane-changing (LC) concentration problem, causes a bottleneck around the merge gore area which can lead to congestion. Mai *et al.* (2016) proposed a C-ITS advisory control strategy that involved an individual driver advisory to distribute lane changes along a freeway weaving segment to alleviate the LC concentration problem. The individual driver advisory used fixed proportions to distribute lane changes by weaving vehicles. However, their study did not focus on finding the optimal solution for

* Corresponding author. Tel.: +61-413-708-441

E-mail address: david.sulejic@hdr.qut.edu.au

the LC distribution. This paper presents an algorithm, based on particle swarm optimisation, to improve the traffic performance on a freeway weaving segment by optimising the LC distribution while satisfying the constraints of the problem.

The objective in an optimisation problem is to find the optimal solution by using some optimisation technique. Applications of heuristic search algorithms inspired by natural phenomena are rapidly growing in diverse scientific fields to solve tough optimisation problems. Researchers have successfully applied heuristic algorithms to a wide variety of civil engineering optimisation problems because heuristic algorithms are not problem-specific, do not require the objective function to be continuous or differentiable (unlike gradient-based optimisation algorithms like the quasi-Newton method), can incorporate constraints, can search vast spaces of candidate solutions (Gopalakrishnan *et al.*, 2013). Heuristic algorithms find quality solutions to tough optimisation problems in a reasonable amount of time, but there is no guarantee that optimal solutions are reached (Yang, 2010). Heuristic algorithms are characterised by some balance between exploration (global search) and exploitation (local search).

Heuristic algorithms are preferred for problems that require good quality solutions which are easily attained, rather than the best solutions. A heuristic algorithm is suited specifically for the lane-changing concentration problem because the individual driver advisory only requires a good quality solution to improve the fitness function. This is more important than the guarantee of an optimal solution because of the relatively high cost in computational effort, to attain the best solution, compared to the marginal improvement in the fitness function.

Many modern heuristic algorithms that have been developed for computer science research: for example simulated annealing, tabu search, genetic algorithms, ant colony optimisation, bee algorithms, differential evolution, particle swarm optimisation, harmony search, big bang-big crunch, the firefly algorithm, cuckoo search and bat-inspired algorithms.

Nature-inspired algorithms are based on the behaviour of so-called swarm intelligence, which forms the foundation of heuristics (Yang, 2014). This research focuses on using swarm intelligence models, mainly PSO, to solve the optimisation problem.

1.1. Particle swarm optimisation

PSO, a heuristic algorithm, has become one of the most widely used algorithms based on swarm intelligence due to its simplicity and flexibility (Yang, 2014). It is a stochastic search and optimisation technique that has been applied to many problem domains which are difficult to solve by conventional methods.

The PSO concept, originally introduced by Eberhart and Kennedy (1995), was inspired by the social behaviour of bird flocking or fish schooling. In PSO, a problem is optimised by iteratively trying to improve a potential solution with respect to an objective function. It solves a problem by having a swarm of particles, or population of potential solutions, which are flown in a high-dimensional search space. Each particle has an adaptable velocity, according to which it flies through the solution space. The movement of the particle is updated according to its own best position in history, and to the current global best position, which is found by the swarm, at the same time it tends to move randomly. When a particle finds a location better than any previously found, it updates that location as the new current best for the particle. The swarm of particles is expected to fly toward an optimal solution through the feasible solution space.

The original PSO algorithm has two variants: global best, *gbest*, and local best, *lbest*, PSO. The global variant, widely used in literature, is used in this research (Gopalakrishnan *et al.*, 2013). Hence, the following describes the global best PSO algorithm.

Consider a D -dimensional search space, where the i th particle of a swarm can be represented by a D -dimensional vector, $X_i = (x_{i1}, x_{i2}, \dots, x_{iD})^T$. The *velocity* of the particle can be represented by a D -dimensional velocity vector $V_i = (v_{i1}, v_{i2}, \dots, v_{iD})^T$. The particle, x_i , has a memory of its previously visited personal best position, denoted as $y_i = (y_{i1}, y_{i2}, \dots, y_{iD})^T$. The social information is the best position found by the swarm, referred to as \hat{y} . Let t denote discrete time steps or the iteration number. Each particle updates its position based on its own best experience, the best

swarm overall experience, and its previous velocity vector, according to equations 1 and 2 (Eberhart and Kennedy, 1995).

$$v_{ij}^{t+1} = \omega v_{ij}^t + c_1 r_{1j}^t (y_{ij}^t - x_{ij}^t) + c_2 r_{2j}^t (y_j^t - x_{ij}^t) \quad (1)$$

$$x_{ij}^{t+1} = v_{ij}^{t+1} + x_{ij}^t \quad (2)$$

where $j = 1, 2, \dots, D$; $i = 1, 2, \dots, n_s$ and n_s is the size of the swarm. The stochastic nature of the algorithm is determined by $r_{1j}^t, r_{2j}^t \sim U(0, 1)$, which are random values, sampled from a uniform distribution in the range $[0, 1]$. These random numbers are scaled by acceleration coefficients c_1 and c_2 , called cognitive and social parameters, respectively, where $0 \leq c_1, c_2 \leq 2$. The performance of each particle is measured by the objective function, which is related to the problem under consideration. The inertia weight ω was added by Shi and Eberhart (1998) to improve the convergence rate. Gopalakrishnan *et al.* (2013) added a maximum velocity parameter, v_{max} , to improve the efficiency of the PSO in the region of the optimum by allowing a finer step-size velocity.

The termination criterion for the PSO can be one of the following: a fixed number of iterations, the maximum number of iterations without improvement, and the minimum error requirement in the objective function.

The swarm behaviour in basic PSO is influenced by the number of particles, the inertia weight, the maximum velocity, and the acceleration coefficients to modify the velocity. These parameters are considered for the speed, convergence and efficiency of the algorithm. The influence of the previous velocity on the current velocity, which affects the trade-off between exploration (global search) and exploitation (local search), can be controlled by the inertia weight, ω . A larger inertia weight facilitates the exploration; a smaller inertia weight tends to facilitate the exploitation of the current search area. Hence, a suitable selection of the inertia weight achieves the right balance between exploration and exploitation (Shi and Eberhart, 1998).

There are several key advantages of PSO over other optimisation techniques: derivative-free algorithm unlike many conventional techniques, only a few parameters to adjust, ability to handle objective functions with stochastic nature, ease of implementation, does not require a decent initial solution to start its iteration process (AlRashidi and El-Hawary, 2009). Since its original development, PSO has been modified into many different variants (Gopalakrishnan *et al.*, 2013). As a heuristic algorithm, PSO does not guarantee to find the optimum solution; therefore, the practitioner may need to modify the algorithm to work efficiently for a given problem.

1.2. Particle swarm optimisation: traffic and transportation engineering applications

Swarm intelligence techniques, including PSO, have been successfully applied for transportation and traffic engineering applications, including transportation network design, traffic flow forecasting, traffic control, traffic accident forecasting and vehicle routing problem (Teodorović, 2008; Gopalakrishnan *et al.*, 2013).

Srinivasan and Seow (2003) proposed a new approach to automatic incident detection on traffic highways using PSO. Their research used PSO to train a neural network in place of back-propagation. The simulation results show that PSO performed better than the back-propagation algorithm.

The vehicle routing problem with time windows accounts for a significant portion of the work of many distribution and transportation systems. Zhu *et al.* (2006) developed an algorithm, based on the principles of PSO, for the vehicle routing problem. The authors tested the proposed approach on a few numerical experiments and compared the results with the results obtained by the genetic algorithm approach. The PSO algorithm discovered optimal solutions in 82% of cases, while the genetic algorithm discovered optimal solutions in 36% of cases. The simulated results indicated that the PSO algorithm could efficiently and quickly achieve a resolution to the vehicle routing problem.

Traffic flow forecasting is a key problem in the real-time adaptive control of urban traffic. Zhao *et al.* (2006) proposed the radial basic function and neural network based forecasting model for two adjacent intersections. They used PSO algorithm to optimise the hidden layer and the output layer weights of the forecasting model. The proposed approach enhanced the training speed and accuracy of the traffic flow forecast.

Chen and Xu (2006) proposed a PSO algorithm for solving the traffic optimisation problem by optimising the average delay and the average number of stops for adjacent junctions. The simulation results showed that the delay per vehicle could be substantially reduced under constant traffic demands and time-varying traffic demands.

Dong *et al.* (2006) proposed a chaos-PSO algorithm, which is a modified PSO algorithm to allow chaotic searching, used to optimise the signal timing for urban area traffic control. The experimental results for traffic networks consisting of nine intersections showed that signal timing optimisation based on chaos-PSO could reduce average delay per vehicle by 41.6%.

Wang *et al.* (2007) used a modified PSO for optimal coordination of the traffic signals in a simulated artery system.

Peng *et al.* (2009) introduced isolation niches embedded in PSO for traffic lights control. The proposed algorithm was used to optimise the time of green and red lights to make the average waiting time for vehicles shorter. The simulation results showed that it was a valid method.

Lianyu *et al.* (2009) proposed a method based on a quantum-behaved PSO algorithm to obtain optimal origin–destination (OD) matrix calculation used in urban traffic management and control.

Kachroudi and Bhouri (2009) proposed an urban traffic control strategy that uses traffic lights to regulate private vehicle traffic and the progression of public transport vehicles. The authors used a modified PSO algorithm to optimise the multi-modal traffic responsive strategy on a large virtual urban network.

Cao *et al.* (2010) proposed a two-direction green wave control algorithm of the traffic signal based on PSO. The PSO optimised the signal split and the phase offset. The simulation result, using traffic data collected from Liansheng Road and Dongguan City, showed the method significantly reduced average delay and average queue length.

Lertworawanich (2012) proposed a PSO algorithm for the sequential highway network recovery problems. The study used a model to determine the optimal highway network restoration sequence after disasters.

These results from research have shown that the PSO is a promising technique capable of solving complex traffic and transportation problems. As there have been few studies relating to the use of PSO in freeway traffic control, this research aims to use PSO algorithm in the lane-changing optimisation problem in a freeway weaving segment.

In a previous study by Mai *et al.* (2016), the distribution percentage was fixed, and optimal solutions were not explored using sophisticated optimisation techniques. This study involves particle swarm optimisation to seek optimal solutions for the LC advisory distribution.

A methodology for the optimisation of the LC advisory distribution is proposed in this section. The proposed algorithm is discussed in further detail below.

Table 1 summarises the notations used in this section.

The basic PSO algorithm (summarised in algorithm 1) needed to be modified to handle the constraints in the optimisation problem. Accordingly, section 2 provides the proposed extension to the basic PSO.

2. Proposed PSO

The PSO algorithm was modified to generate solutions for the LC advisory distribution. Genetic algorithms were attempted for this problem, but the crossover and mutation functions proved difficult when dealing with the given constraints. Conversely, PSO could iteratively improve each decision variable in the potential solution while remaining within the feasible search space. Hence, a PSO algorithm was proposed for this problem because the fitness evaluations could be used to guide the search directly (Paquet and Engelbrecht, 2003). Because the problem could be defined as a continuous optimisation problem with constraints, PSO was a suitable algorithm.

The proposed PSO, for a constrained optimisation problem, has been adapted to search within the feasible solution space. Constraints, in heuristic algorithms, may cause the search to compromise on the optimal solution by just seeking a feasible solution Coello and Montes (2002). So the PSO algorithm needs a mechanism to deal with the constraints of the problem while maintaining its focus on optimisation.

PSO proved to be a useful algorithm to optimise unconstrained functions; however, if some constraints were added to the objective function, the problem became more complicated (Paquet and Engelbrecht, 2003). A modified PSO

Table 1. Notations of parameters and variables

<i>PSO parameters</i>	
$f(x)$	Function to minimise
S	Total number of particles in the swarm
D	Number of dimensions in a particle
i	Index for particle in swarm, S
j	Index for dimension in particle, x_i
x_i	Particle representing a potential solution, $x_i \in \mathfrak{R}^n$
x_{lb}	Lower bound limit for x_{ij}
x_{ub}	Upper bound limit for x_{ij}
ω	Inertia weight, $\omega = 0.7$
ϕ_p	Cognition parameter, $\phi_p = 1.4$
ϕ_g	Social parameter, $\phi_g = 1.4$
$v_i(t)$	Velocity vector, $v_i \in \mathfrak{R}^n$
v_c	Velocity clamping, $v_c = 0.2$
<i>Objective Function</i>	
S	Minimum detector speed
M	Missed turns penalty factor

Algorithm 1: The pseudocode of basic particle swarm optimisation**Input:** PSO parameters**Result:** The best particle found by the algorithm.

```

1 for each particle  $i = 1, \dots, n_s$  do
2   | Initialise particle's position and velocity
3 end
4 while maximum iterations or stopping criteria is not met do
5   | for each particle  $i = 1, \dots, n_s$  do
6     | Calculate fitness value
7     | if the fitness value is better than the best fitness value ( $p_{best}$ ) in history then
8       | |  $p_{best} =$  fitness value
9     | end
10  | end
11  | Choose the particle with best fitness value of all the particles as the  $g_{best}$ 
12  | for each particle  $i = 1, \dots, n_s$  do
13    | Calculate particle velocity according to equation 1
14    | Update particle position according to equation 2
15  | end
16 end

```

algorithm was developed specifically to include the constraints in the optimisation problem. The following sections outline the modifications to the basic PSO.

2.1. Solution representation

To optimise the LC-advisory distribution, the potential solution must be encoded in a suitable form, such as a one-dimensional array jointly comprising the RF and FR LC advisory distributions. Figure 1 depicts a simple potential solution.

RF								FR							
x_{RF_1}	x_{RF_2}	x_{RF_3}	x_{RF_4}	x_{RF_5}	x_{RF_6}	x_{RF_7}	x_{RF_8}	x_{FR_1}	x_{FR_2}	x_{FR_3}	x_{FR_4}	x_{FR_5}	x_{FR_6}	x_{FR_7}	x_{FR_8}

Fig. 1. Solution representation

2.2. Co-evolutionary optimisation

A decomposition approach was implemented to improve the potential solution iteratively. The proposed PSO improved the potential solutions by improving the lane-changing advisory distribution made up of the RF and FR distributions.

Figure 2 provides an example of the steps for this co-evolutionary optimisation approach. Assume there is a swarm size of ten particles, each with 16 decision variables, each column representing one dimension (one decision variable); the swarm of solutions (particles) will be a matrix of $D \times S$ (16×10), as shown in step 1. In the matrix, each row represents one solution (particle), the columns represent the set of decision variables. The initial population is randomly generated within the predefined constraints.

The set of decision variables is divided into the RF and FR subset arrays in step 2; these are denoted by the yellow and green colour, respectively. The size of each subset is $D/2$ ($16/2 = 8$), that is, each subset contains 8 decision variables represented by columns and ten particles (solutions) represented by rows.

The solution vector, created in step 3, is used for the fitness calculation process. The solution vector contains two parts selected from the created subsets, as shown in step 3. In this example, the RF distribution is selected from the first subset array; the FR distribution is selected from the second subset. Each part represents the best solution in its subset. For example, after an iteration, the best solution in the first subset is Individual 5 (highlighted by a black colour), which is used to represent the first part of the solution vector, and Individual 2 from the second subset is used to represent the second part of the solution. Every particle (individual) in a subset is evaluated by combining it with all the best individuals in the solution vector. That is, the solution vector is fed into the objective function for fitness calculation. This is the co-evolutionary process for the PSO algorithm. For example, to calculate the fitness values of all particles in the first swarm, each particle from the first subset is sent to be used as the first part, combined with the second part of the FR subset, and then it is sent to the fitness function to calculate the fitness value of this particle. The same process is repeated for the RF subset. The parts – the best individuals in each subset of the solution vector – are updated during the optimisation process.

The optimisation process (PSO) is called in step 4 to solve each subset separately. Each PSO operates on each subset of solutions and, during the optimisation process of PSO, the fitness value of the newly generated solution are calculated by sending it into the solution vector. The same process is repeated for the second subset.

Figure 3 shows the PSO cycle used to solve the two subsets (denoted as Swarm 1 and Swarm 2). In the first cycle, the PSO process for Swarm 1 is executed, while the representative (global best) from Swarm 2 is sent to form the second part of the solution vector. During the first cycle, the PSO sends each particle into the solution vector and obtains the fitness value. The first cycle will terminate after all particles in Swarm 1 have been evaluated. The search then executes the second cycle to optimise Swarm 2 and uses the representative (global best) from Swarm 1 in the solution vector. Once the second cycle terminates, the search repeats the cyclical process. The process iteratively improves the search for the best solution by updating the current best particle of each swarm.

2.3. Initialisation

The potential solutions were randomly initialised within the feasible domain. The particle's position was initialised using equation 3; it was then transformed within the feasible domain using equation 4.

$$x_{ij} = x_{lb} + r_{ij} \times (x_{ub} - x_{lb}), \quad \forall j = 1, \dots, n_x, \quad \forall i = 1, \dots, n_s \quad (3)$$

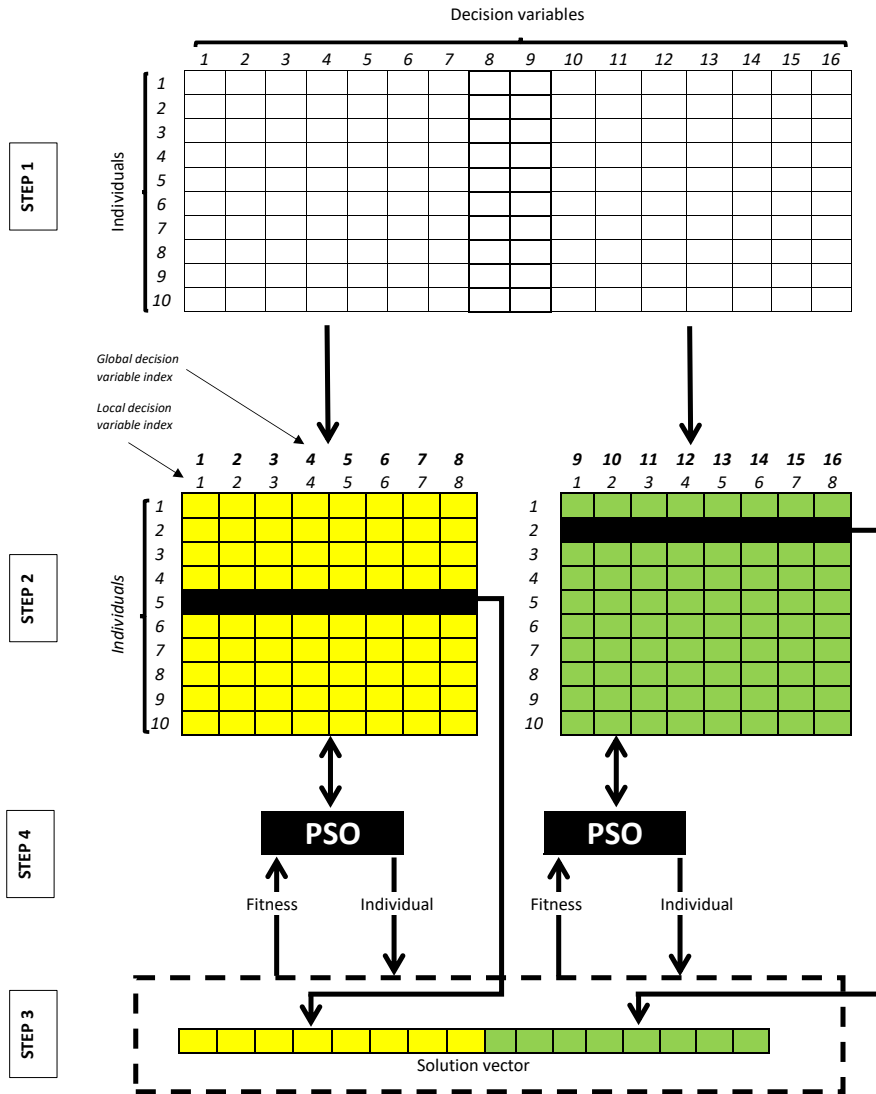


Fig. 2. Co-evolutionary optimisation method

where $r_{ij} \sim U(0, 1)$ and x_{ij} is the position of x for j in n_x dimensions and i in n_s particles. The random variable, r_{ij} , is uniformly distributed between 0 and 1. The lower and upper bounds of position x_{ij} are x_{lb} and x_{ub} , respectively.

$$x'_{ij} = \frac{x_{ij}}{\sum_{j=1}^{n_x} x_{ij}}, \quad \forall j = 1, \dots, n_x, \forall i = 1, \dots, n_s \quad (4)$$

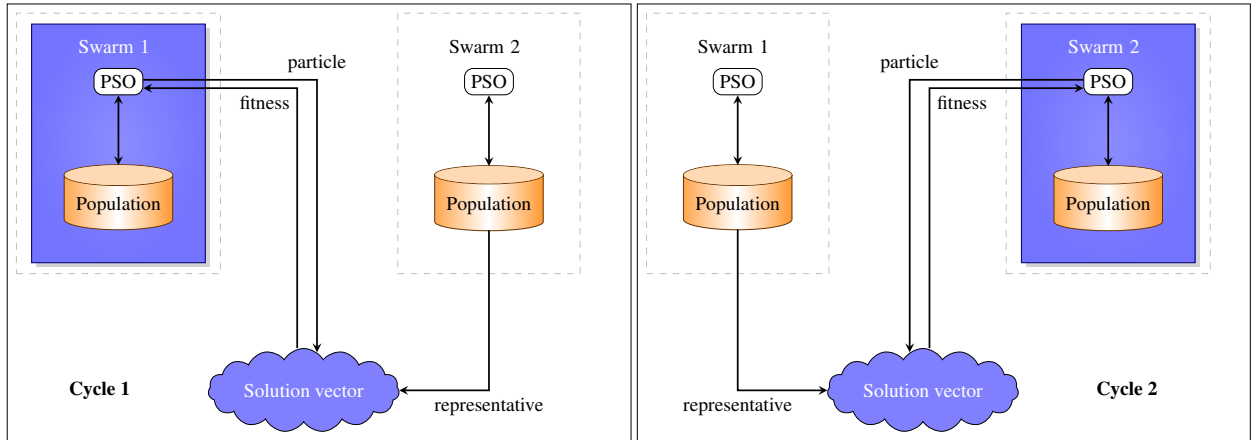


Fig. 3. PSO cycle process

where x'_{ij} is the transformed position, within the feasible space, of x for j in n dimensions and i in S particles. For all j in n dimensions, the position is divided by the sum of values in particle i . This post-processing method was used to initialise positions within the feasible domain.

2.4. Objective function

The problem can be defined as a constrained numerical optimisation problem that seeks to find x , which minimises $f(x)$. This section describes the objective function formulation. The proposed PSO algorithm inputs the LC advisory distribution, x , into Aimsun, which outputs the fitness evaluation (see figure 4). The problem will be optimised by iteratively trying to improve a potential solution for the objective function.

In this work, the objective function consisted of two parts: speed and missed turns. The speed was measured in the conflict area of the weaving segment, where most of the turbulence typically occurred due to merging and diverging traffic streams. In this study, the auxiliary lane and lane 3 experienced the most LC turbulence between merging and diverging vehicles; consequently, speed along these lanes was used as an indicator of traffic flow dynamics, how smoothly vehicles drove through the segment. The speed was measured by detectors that were spaced at 10-m intervals. This study used 1-minute aggregation for all detector measurements. The detector with the minimum speed measurement would represent the point where speed drop was most significant. Denny and Williams (2005) found that the speed would be the lowest close to the merge gore areas where the maximum interaction between merging and diverging vehicles occurred because of the bottleneck formation. Hence, regarding the objective function, it was pertinent to increase the minimum speed and to reduce speed drop caused by a LC concentration. The minimum speed, measured at a detector, would be substituted into the objective function.

Missed turns occurred when a weaving vehicle was unable to perform its required lane change before the end of the segment; thus, missing its desired turn or exit leg. This tended to occur when vehicles were assigned a section close to the end of the diverging point, and no suitable gap was found to change lanes. This is undesirable for drivers and should be avoided. Hence, in this study, missed turns have been penalised by a factor, M , shown in equation 6.

The LC distribution was optimised based on the objective function, summarised in equation 5. The free-flow speeds for the freeway and on/off ramps were 100 km/h and 80 km/h, respectively.

$$\min f(x) = \frac{1}{S} + M \quad (5)$$

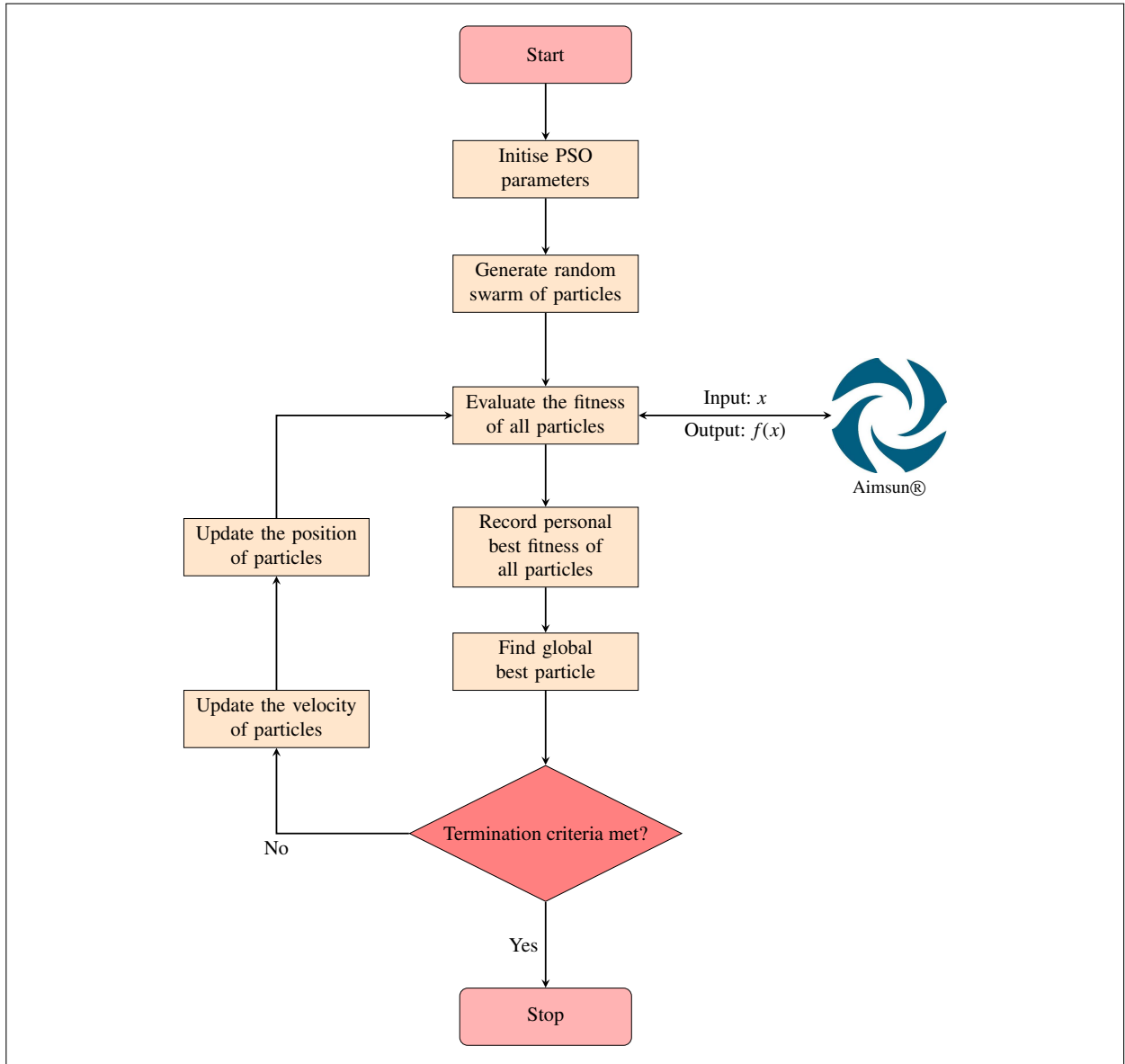


Fig. 4. The flowchart of PSO

where $f(x)$ is the objective function for a given LC distribution, x_i , S is the value derived from the speed detector measurements, and M is the penalty factor for the number of missed turns. M is a weighted penalty factor that is expressed as:

$$M = N + m^2 \tag{6}$$

where N is a user-defined constant and m is the number of missed turns. The number of missed turns, m , is defined as the number of vehicles that are unable to find a gap in time to proceed to their desired exit. The factor has been squared to increasingly penalise this undesirable outcome.

The proposed PSO was used to improve the LC concentration problem by optimising the LC advisory distribution.

2.5. Constraints

The optimisation problem includes both boundary and summation constraints. These set of constraints is imposed by conditions that the variable, x , must satisfy to find a feasible solution. These constraints are presented in equations 7 and 8.

$$\sum_{j=1}^{n_x} x_{ij} = X, \quad \forall i = 1, \dots, n_s \quad (7)$$

where X is the value for feasible solutions, as defined by the linear constraint on the LC-advisory distribution.

$$x_{lb} \leq x_{ij} \leq x_{ub}, \quad \forall j = 1, \dots, n_x, \forall i = 1, \dots, n_s \quad (8)$$

where x_{lb} and x_{ub} are the lower and upper bound values, respectively.

2.6. Velocity

The basic PSO algorithm updated the position of its particles with a velocity equation that was unconstrained. A constraint handling mechanism was used to guarantee a feasible solution.

The basic velocity equation was implemented, then a constraint-preserving method was applied to ensure that the particle's position satisfied the constraints. In this process, where decision variables have violated the boundary constraint, the violation was discretely distributed across dimensions which may satisfy the boundary constraint.

Velocity clamping was also implemented to control the exploration of particles within the boundary constraints. If a particle's velocity exceeded the specified maximum velocity, the particle's velocity was set to the maximum velocity (Engelbrecht, 2007).

2.7. Position

Based on the calculated velocity, the updated position remains within the feasible domain. The positions of all particles are updated using equation 2.

2.8. Termination criteria

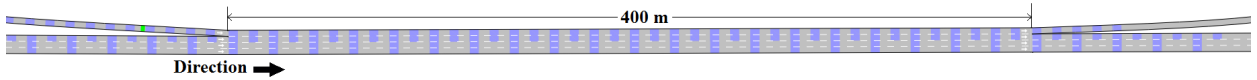
Iterations of the algorithm are executed until a stopping condition is satisfied. In this work, the criterion was set to a maximum of 50 iterations.

3. Case Study

This section covers the microscopic traffic simulation set-up, including the network configuration and simulation settings; the performance indicators used for evaluation; and finally, the results and discussions.



(a) M60 Motorway aerial image



(b) M60 Aimsun network

Fig. 5. M60 Motorway test bed

3.1. Simulation test bed

Traffic simulation has been used to evaluate the application of the C-ITS lane-changing advisory and the implementation of the optimisation algorithm.

The model was built using a commercially available microscopic traffic simulation software, AIMSUN (advanced interactive microscopic for urban and non-urban network), which was developed by Transportation Simulation Systems (TSS) in Spain (Barceló, 2010). Aimsun contains a microscopic simulator and offers an API with its microsimulation software. This study used the API, which enables Aimsun to interface with external applications, the development language Python, and version 8.1.5 of Aimsun.

The simulation period is 15 minutes, with a 10-minute warm-up period. Each test scenario runs 20 replications to capture the stochastic variation in traffic flow. The average of the 20 simulation runs was used for output analysis.

An empirical study, by (Al-Jameel, 2013), examined the characteristics of driver behaviour in weaving segments using field data extracted from video recordings of seven motorway weaving sites. This study used the existing network based on the M60 Motorway (Manchester City, UK). This segment was coded in a previous study by Mai *et al.* (2016).

The network, a short weaving segment with a length of 400 m, has a width of four continuous lanes: three freeway-to-freeway lanes and a one-lane, left-side on-ramp, followed closely by a one-lane, left-side off-ramp. The two ramps are connected by a continuous freeway auxiliary lane. The configuration, defined as a one-sided weaving segment, requires no more than two completed lane changes. The speeds are coded as 100km/h and 80km/h for the freeway and ramp sections, respectively. The geometry of the weaving segment is shown in figure 5 (considering left-hand side traffic direction).

The demand data for the weaving segment were taken from study by Al-Jameel (2013). The model, which considered only cars in its traffic composition, had the following demand flow rates:

- FF demand flow: 5300 veh/h
- RF demand flow: 900 veh/h
- FR demand flow: 900 veh/h
- RR demand flow: 100 veh/h

The model calibration and validation processes were undertaken in a previous study by Mai *et al.* (2016). In their study, they calibrated the lane-changing model by adjusting the ‘distance to zone’ parameters, which represented the lane-changing motivation characteristics. Their model, which uses the observed data from an empirical study by Al-Jameel (2013), calibrates and validates the high lane-changing concentration problem to represent weaving behaviour accurately. Hence, their model can be used reasonably for a comprehensive analysis of different test scenarios. Table 2 lists the parameters describing the weaving segment.

Table 2. Weaving segment parameters

v_{FF}	=	freeway-to-freeway flow rate in the weaving segment (veh/h)
v_{RF}	=	ramp-to-freeway flow rate in the weaving segment (veh/h)
v_{FR}	=	freeway-to-ramp flow rate in the weaving segment (veh/h)
v_{RR}	=	ramp-to-ramp flow rate in the weaving segment (veh/h)
v_W	=	weaving demand flow rate in the weaving segment (veh/h), $v_W = v_{RF} + v_{FR}$
v_{NW}	=	weaving demand flow rate in the weaving segment (veh/h), $v_{NW} = v_{FF} + v_{RR}$
v	=	total demand flow rate in the weaving segment (veh/h), $v = v_W + v_{NW}$
N	=	number of lanes within the weaving segment, $N = 4$
L	=	length of the weaving segment (m), $L = 400$
RF-ratio	=	ramp-to-freeway volume ratio, v_{RF}/v_W

3.2. Performance indicators

Performance indicators, or measures of effectiveness, need to be carefully chosen to evaluate the weaving segment. Average speed is commonly used as an operational indicator; however, Cassidy and May (1991) found that it does not reliably reflect operational quality in a weaving segment. Cassidy *et al.* (1989) observed that speed appears to be insensitive to low and moderate conditions. Denny and Williams (2005) found that the speed would be the lowest close to the merge gore areas, where the maximum interaction between merging and diverging vehicles occurred because of the bottleneck formation. The speed would increase once the vehicles moved through the bottleneck location. Hence, speed will not be used as an operational performance indicator in this research. Instead, speed will show the traffic flow dynamics, how smoothly drivers travel through the weaving segment and whether the LC concentration problem has been alleviated.

Detectors, spaced at 10m intervals, collected speed measurements. This research used 1-minute aggregation for all detector measurements. The detector speed measurements can be used to show the speed profile along the weaving segment and to plot the speed contours.

Two performance indicators were used to evaluate the weaving segment and to compare the optimised case and the base case: average vehicular delay and time savings.

Aimsun recorded the average delay, calculated as the difference between the actual travel time and the free-flow travel time. The free-flow travel times of the mainline vehicles (FF and FR) and the on-ramp vehicles (RF and RR) were calculated at speeds of 100 km/h and 80 km/h for the freeway lanes and ramps, respectively. For mainline vehicles, the actual travel time was recorded from 500 m upstream of the merge gore to downstream of the weaving segment. For on-ramp vehicles, the travel time is recorded from 130 m from the merge gore to downstream of the weaving segment. The unit of average delay time was measured in seconds per vehicle (s/veh). The time saving (s/veh) was used, as another performance indicator, to indicate the travel time savings achieved by the advisory control strategy.

4. Evaluation of the proposed PSO algorithm

This section gives an example that demonstrates the performance of the proposed PSO.

The proposed PSO has been modified to handle the constraints of the problem; however, the input parameters are the same as those of the basic PSO.

In all experiments, the inertia weight, ω , was set to 0.7, while the values of ϕ_p and ϕ_g were set to 1.4. When comparing the inertia weights and constriction factors in PSO, Eberhart and Shi (2000) found that these values gave acceptable results. The velocity clamping (v_c) used was 0.2 (higher values were tested; however, this value provided the best results).

The objective function was defined in section 2.4. Function evaluations were performed by passing the potential solution, x , into Aimsun and obtaining a fitness value, $f(x)$. The test example minimises equation 5, subject to the constraints in equation 7.

Table 3 lists the swarm sizes tested to evaluate the performance proposed PSO.

Table 3. Proposed PSO test runs

Run	Number of particles
Run A	10
Run B	20

Figure 6 shows the best fitness values (averaged over five simulations). The results show how the proposed PSO algorithm converges near a local minima. Run A converges after approximately 40 iterations, whereas Run B converges after 30 iterations.

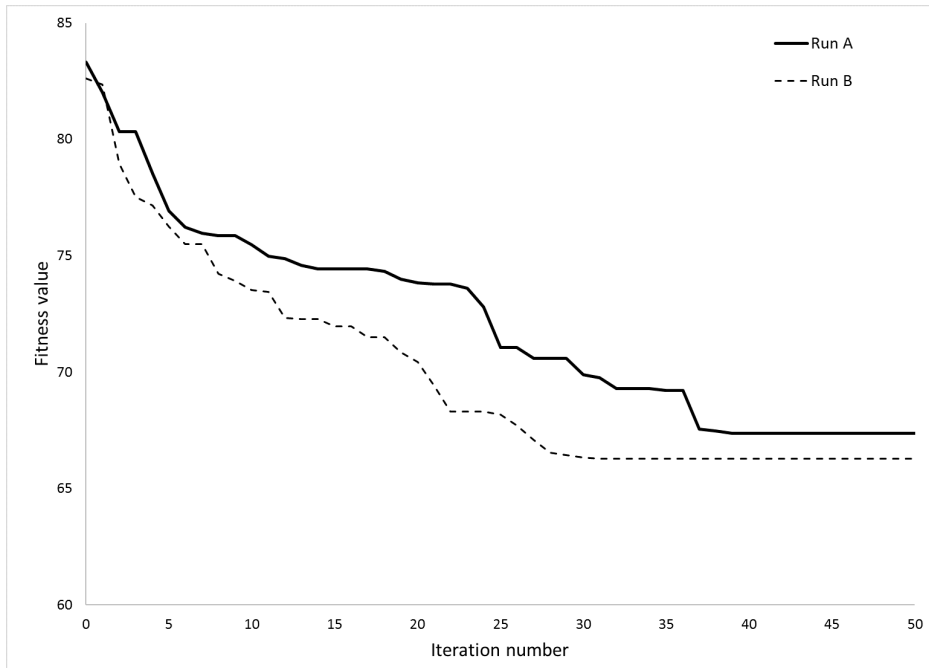


Fig. 6. Proposed PSO results

Table 4 shows the best fitness values at the final iteration (over five simulations). The table also shows the maximum and minimum fitness values at the final iteration, over five simulations. In this example, the results show that the swarm size has a marginal difference to the final fitness value. Hence, to save on computational time, a swarm size of ten was used for all simulation runs.

Table 4. Fitness values

Proposed PSO	Run A	Run B
Average	67.31	66.14
Maximum	71.15	73.26
Minimum	63.18	59.79
Standard Deviation	2.78	5.33

The test example was also used to evaluate the effect of the penalty factor. Initially, the penalty factor was set to zero, meaning that missed turns were not punished in the objective function. The results were as expected, showing that the best LC advisory distribution did not advise vehicles in time to allow them to execute their desired lane change; an average of 25 vehicles missed their exit. When the penalty factor was applied to the objective function, there were no missed turns for the best LC advisory distribution. The penalty factor is therefore imperative to the

objective function, to avoid vehicles missing their exits. In this study, the sensitivity for the penalty factor was not investigated.

The results demonstrate that the proposed PSO algorithm can be reasonably used to optimise the LC advisory distribution.

4.1. Simulation results and discussion

The proposed PSO algorithm found the best LC-advisory distributions. The PSO code was executed using Spyder (The Scientific PYTHON Development EnviRONment) on an Intel® Core™ i7 2.50 GHz processor with 8.0 GB RAM, running on Windows 10, 64-bit Operating System. The computing times for each PSO experiment was approximately six hours. There was no focussed attempt to improve the efficiency of the algorithm for this study.

The best LC advisory distribution, obtained from the proposed PSO algorithm, will be compared with the base case, with no control strategy. To test the strategy, the results are evaluated between the following two cases:

- Base case: no control
- Optimised case: individual driver advisory control strategy (optimised LC advisory distribution)

The base case assumes no control strategy. The LC behaviour is governed by Aimsun's LC model using the calibrated LC parameters. The base case was used as a benchmark for comparison.

The advisory control strategy divides the 400-m weaving segment into eight equal 50-m sections. The RF and FR vehicles are assigned a section, from which they can begin a lane change. In the optimised case, the best LC advisory distribution, found by the proposed PSO algorithm, is applied to the individual driver advisory control strategy.

4.2. Performance evaluation

The test bed, described in Section 3.1, was used as an example to evaluate the performance of the proposed PSO algorithm in optimising the LC advisory distribution. Section 3.1 summarised the traffic demand used for the test case.

Table 5 shows a comparison between the average delay time per vehicle (s/veh) in the base case and the optimised case. The optimised case shows a substantial delay improvement of 30% and 34% for the FF and FR movements, respectively. The delay improvement was 8% and 1% for the RF and RR movement, respectively. On average, for all movements per vehicle, delay significantly improved by 28%.

Table 5. Average delay comparison between base case and optimised case

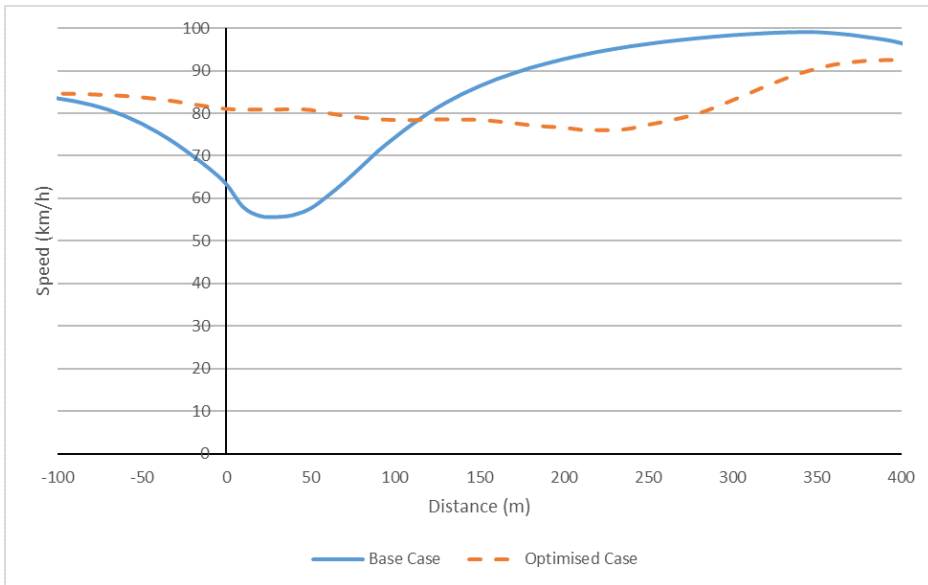
Movement	FF	FR	RF	RR	Average
Traffic volume (veh)	5300	900	900	100	
Expected travel time (s/veh)	52.9	47.1	43.0	37.1	
Delay in base case (s/veh)	12.8	16.5	9.8	5.2	8.8
Delay in optimised case (s/veh)	8.9	10.8	9.0	5.1	6.3
Improvement from base case (%)	30	34	8	1	28
Significance*	0.000	0.000	0.000	0.787	

*The delay difference is significant at the 0.05 level

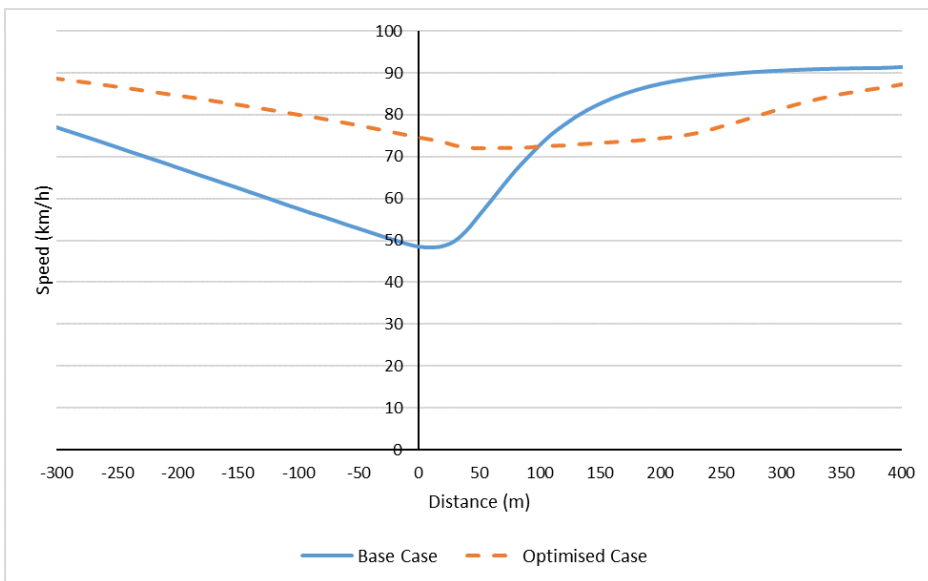
The *t*-test was performed to examine whether the delays for the base case and the optimised case were statistically different. The *t*-test showed that the optimised LC advisory significantly reduced delay for the FF, FR and RF movements in the weaving segment. The difference in delay for the RR movement was not significant.

The average speed over distance was used to show the location of speed drop caused by the LC concentration problem. Figures 7(a) and 7(b) shows the speed over the auxiliary lane and lane 3 distances, respectively. As clearly demonstrated in both graphs, the speed profile from the optimised case shows a considerable reduction in speed drop near the merge gore, which implies that lane changing was effectively distributed along the weaving segment. The base case speed profile shows that speed increases after the speed drop, as vehicles move through the bottleneck location. It is more desirable, with respect to the operational performance, to have a smoother speed curve. Regarding traffic safety, crashes are more likely to occur during high deceleration (high-speed drop) and less likely to occur during

constant speed (Lee *et al.*, 2006). A higher speed difference increases the crash risk, as drivers may have a rear-end crash if distracted or unable to react in time (Wang *et al.*, 2015). Hence, a smoother traffic speed dynamic, which was achieved by the optimised case, is more desirable.



(a) Speed on auxiliary lane



(b) Speed on lane 3

Fig. 7. Speed profile on critical weaving lanes

It can be observed from the simulation analyses that the advisory control strategy, which uses the best LC advisory distribution found by the proposed PSO algorithm, improves the minimum speed at the bottleneck location. This indicates that the proposed algorithm and objective function can be used to optimise the LC advisory distribution and, hence, to improve the operational performance of the weaving segment.

4.3. Impact of different OD demands

This section investigates the impact of different OD demands on the LC distributions. The criteria for OD demand selection, for each scenario, were that the:

- maximum weaving flow of either RF or FR does not exceed 1260 veh/h
- maximum number of passenger cars in the weaving segment is 2200 veh/h/lane.

The tests were conducted using five different OD demands, as shown in table 6. The five OD demands have different RF-ratios, where the FF , RR and total weaving volumes remained the same as in section 4.1. The level of service (LOS) in each scenario was E, according to HCM 2010, chapter 12 (TRB, 2010), which indicates that the weaving segment is approaching congestion – where the demand flow rate exceeds the capacity of the segment. HCM 2010 (TRB, 2010) does not distinguish LOS for different RF-ratios.

Table 6. Different demand setting (veh/h)

Test	v_{RF}	v_{FR}	v_{FF}	Total weaving	v_{RR}	RF ratio
A	540	1260	5300	1800	100	0.3
B	720	1080				0.4
C	900	900				0.5
D	1080	720				0.6
E	1260	540				0.7

The proposed algorithm was used to optimise the LC advisory distribution for the different OD demands. PSO, considered a heuristic algorithm, does not guarantee a unique solution for the optimal LC advisory distribution. However, the optimised LC advisory distribution aims to change the behaviour of the weaving vehicles to alleviate the LC concentration problem by better utilising existing infrastructure and thereby improving the operational performance of the weaving segment.

Figures 8 and 9 show the performance improvement in lane 3 and the auxiliary lane, respectively. These figures consist of sub-figures, in which the RF-ratio increases from bottom to top, and the base case and optimised case are shown on the left and right, respectively. For each sub-figure, the horizontal and vertical axes represent the distance (m), from the merge gore, and time (min), respectively. The shading illustrates the average speed measured over time and distance; the darker shade represents slower speeds and the lighter shade, faster speeds. The following observations have been made from figures 8 and 9:

1. Overall, the optimised case, in each scenario, has a lighter shade in the contour plots, which represents faster speeds along the weaving segment in lane 3 and auxiliary lane, relative to the respective base case.
2. The bottleneck location in the base case, represented by the dark band concentrated near the merge gore, is alleviated in the optimised case. In all optimised cases, the speed is more smoothly distributed across the weaving segment.
3. The gradient of the contours are less steep in the optimised cases than that in the base cases, where the contours are concentrated near the merge gore.
4. In the base case, the speed decrease near the merge gore, caused by the lane changing concentration problem, progressively becomes more severe as the RF-ratio increases.
5. The optimised cases perform better in smoothing the speed over the weaving segment. The contour plots demonstrate that the optimised LC advisory considerably improves how smoothly drivers travel through the weaving segment.

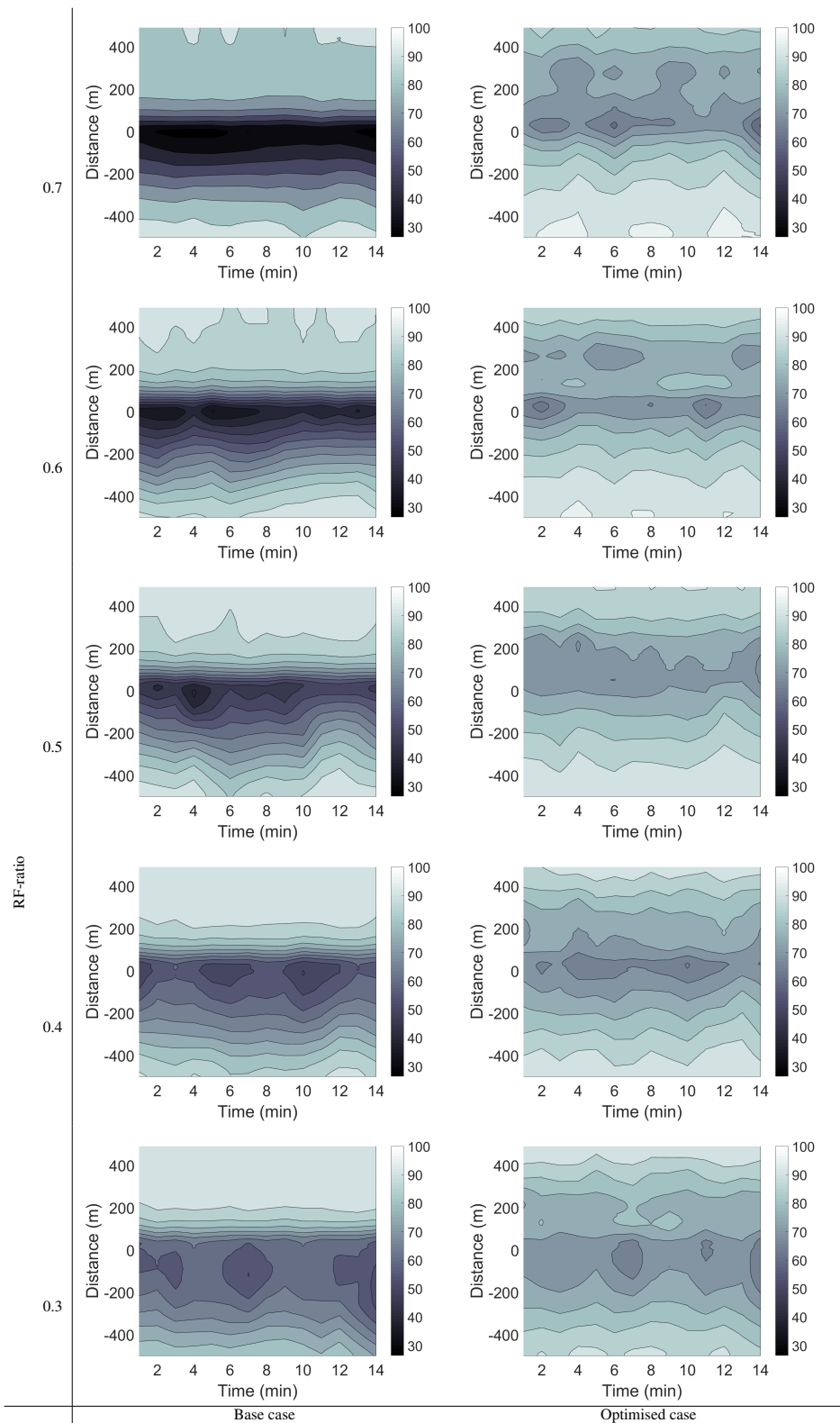


Fig. 8. Contour speeds of lane 3

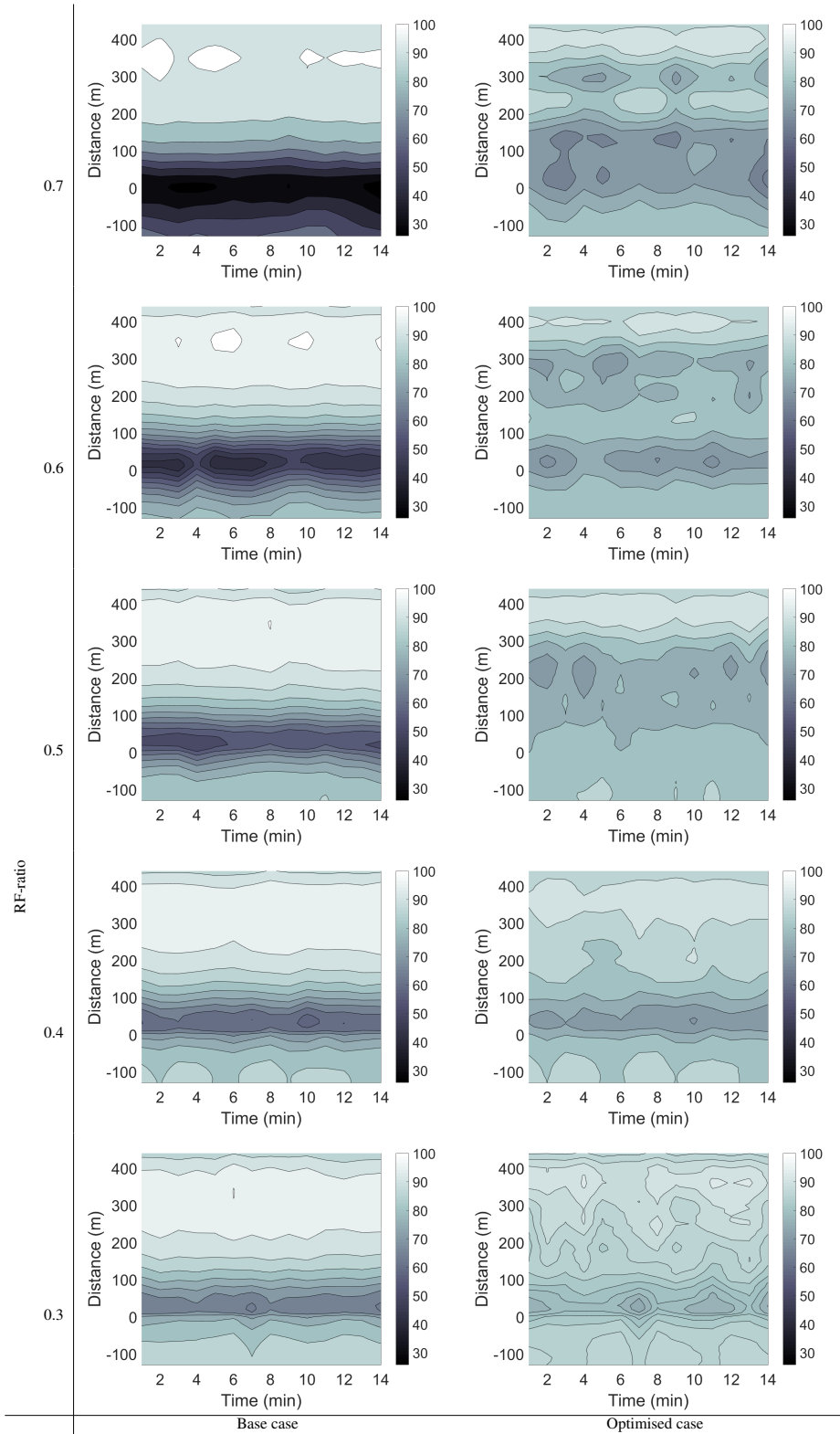


Fig. 9. Contour speeds of auxiliary lane

4.4. Application domain analysis

This section identifies the application domain of the optimised LC-advisory distribution. The LC-advisory distribution was optimised for each scenario. The executed lane changes of weaving vehicles will be analysed for the optimised LC advisory to observe what effect the strategy has on drivers. Before this analysis, the number of lane changes, per section, is examined for the base case (see in table 7).

Table 7. Lane-changing distribution (Base case)

RF-ratio	0.7	RF	882	302	50	13	0	0	0	0	
		FR	378	124	27	5	0	0	0	0	
		Total	1260	427	77	18	0	0	0	0	
	0.6	RF	594	400	54	11	0	0	11	0	
		FR	432	223	43	7	0	0	0	0	
		Total	1026	623	97	18	0	0	11	0	
	0.5	RF	378	432	72	9	0	9	0	0	
		FR	495	324	63	9	9	0	0	0	
		Total	873	756	135	18	9	9	0	0	
	0.4	RF	230	403	72	7	0	0	0	0	
		FR	626	356	76	11	0	0	0	0	
		Total	857	760	148	18	0	0	0	0	
	0.3	RF	162	308	59	5	0	0	0	0	
		FR	806	340	76	13	13	0	0	0	
		Total	968	648	135	18	13	0	0	0	
				1	2	3	4	5	6	7	8
				Section							

From the LC distributions in the base cases, the following observations have been made:

1. The majority of lane changes occur in the first two sections (0-100 m) of the weaving segment.
2. The dominant weaving demand flow movement dominates the number of lane changes in the first segment (0-50 m).
3. The last five sections (150-400 m) of the weaving segment are severely underutilised in all scenarios.

In contrast to the base case, the optimised LC advisory aims to change the LC behaviour of weaving vehicles to achieve better utilisation and to improve the performance of the weaving segment. The simulation records the executed number of lane changes for the optimised LC advisory (see table 8). The number of lane changes per section is recorded for RF and FR vehicles.

Table 8. Lane-changing distribution (optimised case)

RF-ratio	0.7	RF	88	139	340	239	63	113	202	76	
		FR	235	207	72	18	5	2	1	1	
		Total	323	345	412	257	68	116	203	76	
	0.6	RF	108	184	43	119	140	184	227	76	
		FR	301	226	53	34	29	30	31	16	
		Total	409	410	97	153	170	213	257	91	
	0.5	RF	13	68	88	135	230	233	107	26	
		FR	271	216	146	108	81	54	20	4	
		Total	284	285	235	242	311	287	127	30	
	0.4	RF	126	246	119	57	63	69	29	12	
		FR	393	204	108	56	105	84	60	72	
		Total	519	449	227	113	167	153	89	83	
	0.3	RF	59	146	92	65	49	54	54	22	
		FR	542	202	76	113	88	101	88	50	
		Total	601	347	167	178	137	155	142	72	
				1	2	3	4	5	6	7	8
				Section							

From the LC distributions in the optimised cases, the following observations were made:

1. The number of lane changes for weaving vehicles are distributed across all sections of the weaving segment. This indicates that the entire length is being better utilised for LC activity, compared to the base case where it is concentrated in the first two sections.

2. The maximum number of lane changes in a section is considerably lower than that in the base case. This indicates that the LC concentration problem has been alleviated; consequently, LC has been distributed across all sections to avoid high LC density in any given section.
3. Under congested conditions, the volume per lane on the weaving segment is at or close to capacity. Hence, distributing vehicles across lanes at the weaving segment will create gaps for LC. Within the first two sections, in most scenarios, the number of lane changes by FR movements is greater than the RF movement. This indicates that FR vehicles in the congested freeway lane tend to, as soon as possible, change lanes to the less congested auxiliary lane; consequently, reducing the volume in lane 3, which creates greater gap acceptance to facilitate LC for RF vehicles. Priority tends to be given to the FR movement in the first section as there are more gaps in the auxiliary lane to change lanes, thereby, decreasing the volume in lane 3, which creates gaps for the RF movement to change lanes further downstream.
4. In most scenarios, a proportionally high number of lane changes are loaded within the first two sections (0-100 m), then gradually distributed across the remaining sections; the lowest number of lane changes occurred within the final section to avoid missed exits due to overcrowding.

5. Conclusion

In this paper, a PSO algorithm was proposed for a individual driver advisory on a freeway weaving segment. Empirical research has observed that a LC concentration problem occurs in weaving segments close to capacity. The distribution of lane changes was found to be concentrated near the entrance, at times as soon as vehicles enter the segment. This behaviour leads to congestion and reduces the weaving segment capacity. An advisory control strategy was shown to alleviate the problem by distributing lane changes along the entire segment according to fixed distributions. Unlike previous methods, this work proposed an optimisation algorithm, based on PSO, to improve the LC advisory distribution for weaving vehicles. The speed over a short section of the weaving segment, within the critical weaving area, was used as the objective function. Traffic simulation was used to evaluate the performance of the weaving segment using a individual driver advisory and to compare it with the base case, with no control strategy. These conclusions were made from the results:

1. The proposed PSO algorithm can be successfully used to improve the performance of the weaving segment by optimising the LC advisory distribution, given the constraints of the problem. The PSO algorithm was modified to satisfy the boundary and summation constraints implicit in the solution representation.
2. The evaluation of the simulation tests revealed that the optimised LC advisory significantly improved the traffic performance of the weaving segment. The performance indicators, speed and delay, were improved as a result of the optimised LC advisory, with speed producing a smoother profile than that of the base case.
3. The optimised LC advisory was shown to effectively distribute the LC of weaving vehicles across the entire length of the weaving segment. Priority tends to be given to the FR movement in the first section as there are more gaps in the auxiliary lane to change lanes. This decreases the volume in lane 3, which creates gaps for the RF movement to change lanes further downstream.

Although field tests would provide more accurate outcomes, the evaluation of traffic simulation shows improved performance for a weaving segment when optimising the LC advisory distribution. This study concludes that the proposed PSO algorithm can be used to optimise the LC advisory on a freeway weaving segment, resulting in better LC distributions.

Acknowledgements

The author would like to acknowledge the Department of Transport and Main Roads, Queensland, for providing the support to perform this research under the Study and Research Assisted Scheme.

References

- Hamid Al-Jameel. Characteristics of the driver behaviour in weaving sections: empirical study. In *International Journal of Engineering Research and Technology*, volume 2. ESRSA Publications, 2013.
- Mohammed R AlRashidi and Mohamed E El-Hawary. A survey of particle swarm optimization applications in electric power systems. *IEEE Transactions on Evolutionary Computation*, 13(4):913–918, 2009.
- Jaume Barceló. *Fundamentals of traffic simulation*, volume 145. Springer, 2010.
- Cheng Tao Cao, Feng Cui, and Geng Qi Guo. Two-direction green wave control of traffic signal based on particle swarm optimization. In *Applied Mechanics and Materials*, volume 26, pages 507–511. Trans Tech Publ, 2010.
- Michael J Cassidy and Adolf D May. Proposed analytical technique for estimating capacity and level of service of major freeway weaving sections. *Transportation Research Record*, 1320:99–109, 1991.
- Michael Cassidy, Alex Skabardonis, and Adolf D May. Operation of major freeway weaving sections: recent empirical evidence. *Transportation Research Record*, (1225), 1989.
- Juan Chen and Lihong Xu. Road-junction traffic signal timing optimization by an adaptive particle swarm algorithm. In *Control, Automation, Robotics and Vision, 2006. ICARCV'06. 9th International Conference on*, pages 1–7. IEEE, 2006.
- Carlos A C Coello and Efrén Mezura Montes. Constraint-handling in genetic algorithms through the use of dominance-based tournament selection. *Advanced Engineering Informatics*, 16(3):193–203, 2002.
- RW Denny and JC Williams. Capacity and quality of service of weaving zones. *Final Report, NCHRP Project*, pages 3–55, 2005.
- C Dong, Z Liu, and X Liu. Chaos-particle swarm optimization algorithm and its application to urban traffic control. *International Journal of Computer Science and Network Security*, 6(1 B):97–101, 2006.
- Russ C Eberhart and James Kennedy. A new optimizer using particle swarm theory. In *Proceedings of the sixth international symposium on micro machine and human science*, volume 1, pages 39–43. New York, NY, 1995.
- Russ C Eberhart and Yuhui Shi. Comparing inertia weights and constriction factors in particle swarm optimization. In *Evolutionary Computation, 2000. Proceedings of the 2000 Congress on*, volume 1, pages 84–88. IEEE, 2000.
- Andries P Engelbrecht. *Computational intelligence: an introduction*. John Wiley & Sons, 2007.
- Kasthurirangan Gopalakrishnan, AH Gandomi, XS Yang, and S Talatahari. Particle swarm optimization in civil infrastructure systems: state-of-the-art review. In *Metaheuristic applications in structures and infrastructures*, pages 49–76. Elsevier London (UK), 2013.
- Haitao He and Monica Menendez. Empirical comparison between longer and shorter weaving sections in Switzerland. Swiss Transport Research Conference (STRC), 2016.
- Sofiane Kachroudi and Neila Bhourri. A multimodal traffic responsive strategy using particle swarm optimization. *IFAC Proceedings Volumes*, 42(15):531–537, 2009.
- Eil Kwon, Rich Lau, and James Aswegan. Maximum possible weaving volume for effective operations of ramp-weave areas: online estimation. *Transportation Research Record: Journal of the Transportation Research Board*, (1727):132–141, 2000.
- Chris Lee, Bruce Hellinga, and Frank Saccomanno. Evaluation of variable speed limits to improve traffic safety. *Transportation research part C: emerging technologies*, 14(3):213–228, 2006.
- Joon Ho Lee. *Observations on Traffic Behavior in Freeway Weaving Bottlenecks: Empirical Study and Theoretical Modeling*. ProQuest, 2008.
- Ponlathap Lertworawanich. Highway network restoration after the great flood in thailand. *Natural hazards*, 64(1):873–886, 2012.
- WEI Lianyu, DU Jianfu, et al. Research on od matrix calculation based on quantum behaved particle swarm optimization algorithm. *Journal of Software Engineering and Applications*, 2(05):344, 2009.
- Trung Mai, Rui Jiang, and Edward Chung. A Cooperative Intelligent Transport Systems (C-ITS)-based lane-changing advisory for weaving sections. *Journal of Advanced Transportation*, 2016.
- Ulrich Paquet and Andries Petrus Engelbrecht. A new particle swarm optimiser for linearly constrained optimisation. In *Evolutionary Computation, 2003. CEC'03. The 2003 Congress on*, volume 1, pages 227–233. IEEE, 2003.
- Li Peng, Mao-hai Wang, Jia-ping Du, and Gang Luo. Isolation niches particle swarm optimization applied to traffic lights controlling. In *Decision and Control, 2009 held jointly with the 2009 28th Chinese Control Conference. CDC/CCC 2009. Proceedings of the 48th IEEE Conference on*, pages 3318–3322. IEEE, 2009.
- Yuhui Shi and Russell Eberhart. A modified particle swarm optimizer. In *Evolutionary Computation Proceedings, 1998. IEEE World Congress on Computational Intelligence., The 1998 IEEE International Conference on*, pages 69–73. IEEE, 1998.
- Dipti Srinivasan and Tian Hou Seow. Particle swarm inspired evolutionary algorithm (ps-ea) for multiobjective optimization problems. In *Evolutionary Computation, 2003. CEC'03. The 2003 Congress on*, volume 4, pages 2292–2297. IEEE, 2003.
- Dušan Teodorović. Swarm intelligence systems for transportation engineering: Principles and applications. *Transportation Research Part C*, 6(16):651–667, 2008.
- TRB. Highway Capacity Manual 2010. *Transportation Research Board*, 2010.
- ZW Wang, DY Luo, ZX Huang, and Hang Zhang. Optimal coordination of artery system based on modified particle swarm algorithm. *Syst Eng Theor Pract*, 10:165–171, 2007.
- Ling Wang, Mohamed Abdel-Aty, Qi Shi, and Junyoung Park. Real-time crash prediction for expressway weaving segments. *Transportation Research Part C: Emerging Technologies*, 61:1–10, 2015.
- Xin-She Yang. *Nature-inspired metaheuristic algorithms*. Luniver press, 2010.
- Xin-She Yang. *Nature-inspired optimization algorithms*. Elsevier, 2014.
- Jianyu Zhao, Lei Jia, Yuehui Chen, and Xudong Wang. Urban traffic flow forecasting model of double rbf neural network based on pso. In *Intelligent Systems Design and Applications, 2006. ISDA'06. Sixth International Conference on*, volume 1, pages 892–896. IEEE, 2006.

Qing Zhu, Limin Qian, Yingchun Li, and Shanjun Zhu. An improved particle swarm optimization algorithm for vehicle routing problem with time windows. In *Evolutionary Computation, 2006. CEC 2006. IEEE Congress On*, pages 1386–1390. IEEE, 2006.